Journal of the Persian Gulf
(Marine Science)/Vol.1/No.1/September 2010/8/37-44

# Remote Sensing of Tidal Situation by Monitoring Changes in Suspended Sediment Concentration in Surface Waters

Mobasheri, Mohammad Reza

*Remote Sensing Department, KNToosi University of Technology, Tehran, IR Iran*



## Abstract

Collecting information on suspended sediments concentration (SSC) in coastal waters and estuaries is vital for proper management of coastal environments. Traditionally, SSC used to be measured by time consuming and costly point measurements. This method allows the accurate measurement of SSC only for a point in space and time. Remote sensing from air-borne and space-borne sensors have proved to be a useful method for such studies as it provides an instantaneous and synoptic view of sediments that would otherwise be unavailable. The reason for success of remote sensing in such surveys is the strong positive relationship that exists between SSC and remotely sensed spectral radiance. This spectral radiance could be in the sun reflected and/or scattered or thermal terrestrial wavelength band.

To find an algorithm relating SSC to spectral radiance over Bahmansheer River estuary at the North-West of Persian Gulf, a three-month field measurement (April to June 2003) was conducted while we had MODIS sensor on board of Terra over-passed the scene simultaneously. Ninety samples in fifteen trips were collected. Also the environmental parameters such as atmospheric visibility, air and water temperature, current direction and speed at the sampling point, wind speed and humidity were measured simultaneously.

A close correlation between tide and SSC was observed. It is found that in the flood, the width of the turbid area at the estuary decreases while in the ebb, the suspended sediment distribution extends to the deeper region. Change detection by comparison between a base image of high tide/low tide conditions and any image could be used as a tool for detection of tidal conditions. This would be a powerful tool for monitoring erosion at the coastal area and estuaries.

Keywords: *Remote Sensing, Coast, Tide, Ebb, Flood, Suspended Sediment Concentration*

## 1. Introduction

Estuaries are dynamic water bodies characterized by temporal changes that occur over a spectrum of scales, ranging from short-term (hourly) variations driven primarily by tidal currents to long-term (seasonal or interannual) variations caused by changes in meteorological forcing or river discharges (Mishra, 2004; Harris, 1988). Estuaries are also spatially heterogeneous and often have large horizontal (or vertical) gradients in water properties (e.g. salinity, suspended sediments, phytoplankton biomass) that result from local variations in bathymetry, circulation and mixing, or sources/sinks of dissolved and suspended constituents (Mishra, 2004; Green, et al., 2000). Knowledge of mechanisms that cause spatio-temporal heterogeneity in estuaries is based in large part upon the results of

E-mail: Mobasheri@kntu.ac.ir

in situ sampling that is costly (both in time and money) and often inefficient, particularly if sampling is required over a large geographical area and over more than one time scale.

Truly synoptic measurements from boats are nearly impossible in estuaries having rapid (100-200cm/s) tidal currents. If specific properties of estuarine waters can be measured accurately using remote-sensing techniques, then understanding of mechanisms through which physical processes (tidal advection, estuary non-tidal circulation, horizontal dispersion, resuspension) change in dynamic estuary can be improved.

The result is a trapping mechanism that retains suspended particulates in that region of the estuary (null zone) where the landward bottom current converges with the seaward river current.

Large quantities of suspended sediment are characteristic of tide-dominated estuaries. Strong tidal currents continually resuspend fine sediment in the river channels, so that the water column is naturally highly turbid (Mishra, 2004; Raineya et al, 2003; Li et al., 2003; Turner et al.; 1994; Wells, 1995). Quantities of fine and coarse sediment can pool temporarily within the channel, forming tidal sand banks. A zone of abnormally high suspended sediment can occur in many tide-dominated estuaries, known as the 'turbidity maximum' (Raineya et al, 2003; Wells, 1995). This typically transient feature develops as a result of trapping and resuspension of particles, and contributes to the deposition of material in the tidal sand banks. High suspended sediment loads can also lead to a phenomenon known as 'fluid muds', a gel-like accumulation of low density muddy sediment which may be stationary, or mobilized by tidal currents (Raineya et al, 2003; Wells, 1995). Turbidity is especially marked during spring tides, and the location of the turbidity maximum is variable within estuaries, depending on the tidal cycle (spring to neap) and river flow velocity (Semeniuk, 1982). Ebb and flood tides can follow mutually-evasive channels (which periodically migrate), and currents may be powerful enough to cause scouring at the channel base, leaving gravel and bio-clastic debris at the base (Green et al.; 2000, Harris, 1988).

Turbidity is a measure of water clarity or murkiness. It is an optical property that expresses the degree to which light is scattered and absorbed by molecules and particles. Turbidity results from soluble colored organic compounds and suspended particulate matter in the water column. Suspended particulate matter may include clay and silt (e.g. suspended sediment), and detritus and organisms. The availability of multispectral, and now hyperspectral scanner and radar data from aircraft and satellites at high altitudes, along with computer aided analyses, has created a tremendous increase in the quality of the results that can be obtained using remote sensing capabilities. Recent developments in GIS technology, coupled with improved remote sensing technologies, have led to the development of powerful tools capable of distinguishing SSC patterns, sediment dynamics, tidal forces and geomorphological effects of the tidal currents.

## 2. Sampling Area and Data Collection

The 80 km long Bahmansheer River in southwest Iran is parallel to Arvand River which is the border of Iran and Iraq (fig 1). This river carries large amounts of sediments to the Persian Gulf which varies with tide. The tidal current influences the water level even upstream and at the junction of these two rivers about 80 km away from Bahmansheer estuary.

This usually keeps the water in the estuary, turbid for the most of the time. This turbidity may extend up to a few kilometers far from the estuary out into the deeper region where heavier particles settle to the seabed and will not return to the estuary even with the tidal current force.

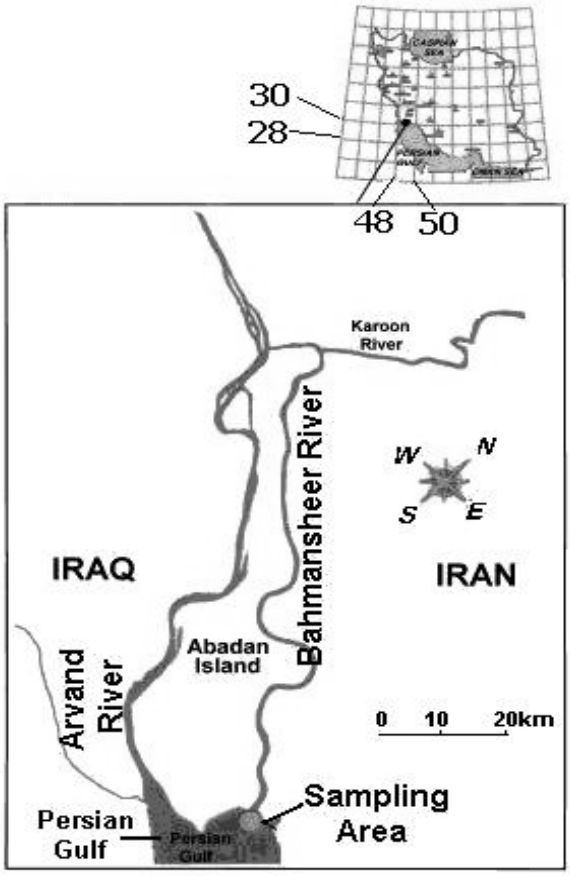


Fig 1. Map of sampling area, northwest of Persian Gulf

Samples were collected simultaneously at the vicinity of the estuary (Fig.1), while MODIS sensor onboard of Terra was passing over the region. Each sample was taken at a minimum distance of 500 meters apart. Along with the sample collection, latitude and longitude were determined using a GPS set. Data on current speed and direction profile (for determination of tidal state), water temperature, wind speed and direction (from the nearest meteorological station) and visibility were collected. These data were used for quality assessment of the images (Mobasheri, 2008). The density of the samples ranged from 30 to 500 mg/lit. Between 1 to 15% of the particles had diameters less than 1µm, consequently Rayliegh scattering was not responsible for the reflection and scattering (Mobasheri, 2006). On the other hand, diameter of more than 45% of the particles was between 0.1 and 9µm. These particles may scatter the visible and near infrared portion of spectrum by Mie scattering (Mobasheri, 2006) that is, channels 1, 2, 3 and 4 of MODIS. The rest of the particles may have nonselective scattering (Mobasheri, 2006). As a result, assumption of a Lambertian reflection for those samples, with low wind speed conditions and high SSC is reasonable (Mobasheri, 2008). Cases where the light was specularly reflected to the sensor was excluded.

It was found that at low tide situation (ebb), the particle size distribution was more towards higher values and as a result an increase of reflections in channels 1, 2 and 4 were detected. All composition content detected in sediment samples were almost translucent to the visible and near infrared portion of the sun spectrum (Mobasheri, 2008). Most of these compositions may be found in building materials and/or minerals.

Fig.(2) is a schematic diagram of the dynamics of the estuary resulting from our in-situ measurements at the four stages starting from a low tide condition, each representing a special case detectable from satellite imageries (from SSC points of view). These:

Stage 1: Fig. (2-a) shows a condition were the low tide stage is present in the area. In this situation, the width of turbid region increases while larger particles may settle down at the interface of fresh and saline water. Depending on the speed profile of water and seabed gradient, water may scour the sedimentation toward the deeper region. Because of strong turbidity a uniform reflectance value could be detected in the images.

Stage 2: Fig. (2-b) shows conditions where ebb converts to flood (beginning of high tide condition). Because of low water speed at this stage, courser particles settle down to the seabed and consequently surface reflectance decreases profoundly. Also thermohaline (salt-freshwater interface) curves toward estuary at the depth, while fresh water rides over saline water towards deeper region. This causes SSC to spread in a wider area on the water surface.

Stage 3: Fig. (2-c) is the next stage where, the high tide condition grows toward estuary and

maximum turbidity due to a strong eddy will commence at the salt-freshwater interface. Some of the sedimentations settled at the previous stages will be washed up at this area while we have sediment deposit at the region closer to the river mouth particularly in channels. In this stage, clear water approaches the river mouth which decreases the width of turbid waters. This creates conditions where the surface reflectance is high with a small SSC gradient toward the sea.

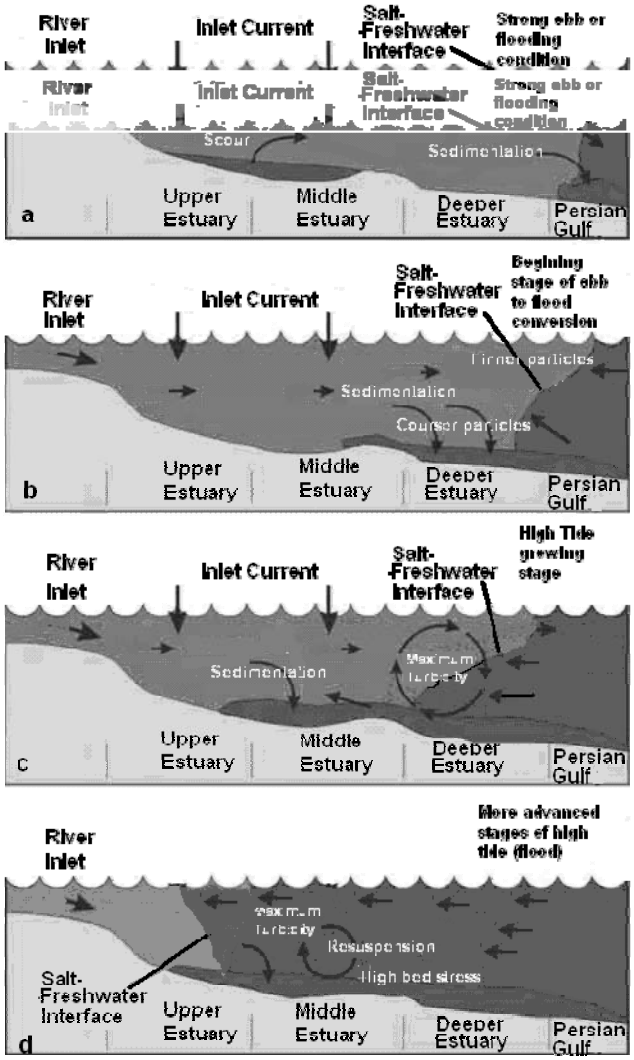


Fig 2. Schematic diagram of the tidal dynamics at the vicinity of Bahmansheer Estuary for four different stages; a-Strong ebb or flooding, b-Stage of ebb to Flood conversion, c-High tide growing stage (flood), d-Mature stage of flood (high tide)

Stage 4: Fig. (2-d) shows the final stages of high tide (flood). At this stage the width of turbid area decreases to its final value. Depending on the seabed slope, this width could vary. As can be seen, maximum turbidity can occur at the vicinity of the seabed, while strong current at the surface will mask this turbidity. This creates an apparent depth shallower than the real one and can be detected by shorter wavelength. Due to the higher penetration of shorter wavelength in the water and their reflection from the seabed, shallow waters (closer to the river mouth) will always look turbid. This turbidity covers all parts of river inland.

## 3. Results and Discussions (use past tense through out the text )

Ten cruises were carried out between April 25th and June 18th, 2003. The data collected were used to produce an algorithm for extracting SSC from MODIS images (Mobasheri, 2008). Three to six sampling points were selected in each expedition. Speed and direction profile in water column were measured along with other parameters for most of the sampling points. This data facilitated the recognition of tidal stage in each cruise. This data, the RGB images supplied by running the afore mentioned algorithm and the SSC indexmay enable one to analyze tidal conditions. Four images, believed to belong to four stages of Fig. (2), were analyzed. In each case current speed and direction at the very surface are shown in figures (3-1) to (3-4) and the relevant images of SSC distribution are shown in figures (5-a) to (5-d). To compare the suspended sediment in recorded in different cruises , images shown in Fig. (4-a) to (4-d) were produced using reflectance $\rho_1$ and $\rho_2$ in channels 1 and 2 of MODIS in the following index (Mobasheri, 2008).

$$SSCI = \frac{(\rho_1 - \rho_2)^2}{\rho_1^2 + \rho_2^2}$$

When water surface was highly turbid there was high reflectance in channel 1 while water constituents (SSC) absorbs in channel 2 and

consequently the index would approach 1. On the other hand, because of atmospheric aerosols, spectral radiance in neither of these two channels gets zero. This index however can mask SSC free waters, land and wetlands, while showing SSC distribution better, and proved to be useful for our study.



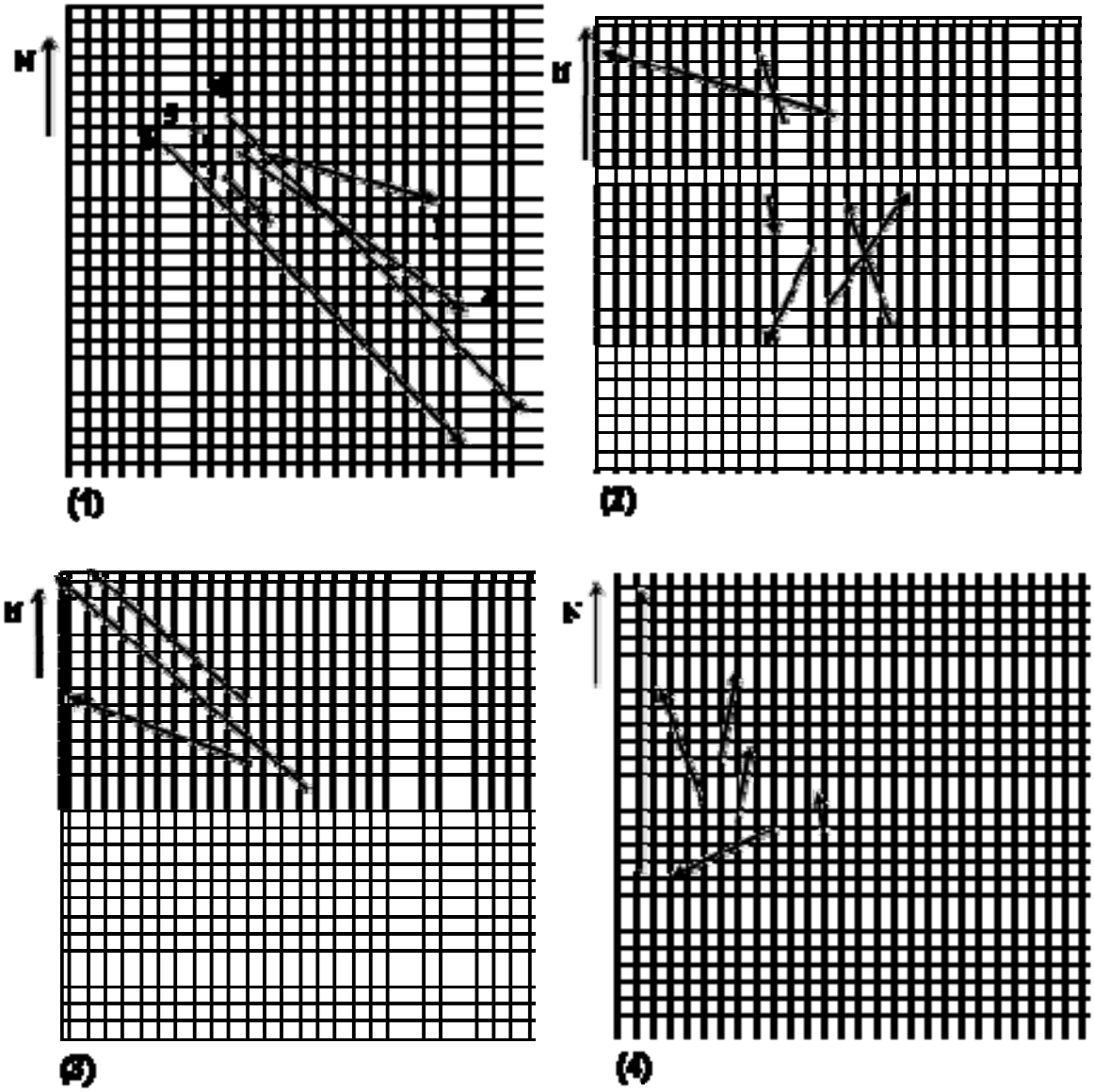

Fig 3. Current speed and direction at the very surface (top 10 cm) (1) 1st expedition (2) 2nd expedition (3) 10th expedition (4) 4th expedition

Table 1-Speed and direction of water at different depth in the first expedition.

| Sampling station no. | Depth (cm) | Direction (degree) | Speed (cm/s) | Sampling station no. | Depth (cm) | Direction (degree) | Speed (cm/s) |
|---|---|---|---|---|---|---|---|
| 1 | 50 | 105 | 28 | 4 | 300 | 135 | 21 |
| 1 | 350 | 150 | 3 | 5 | 40 | 105 | 0 |
| 1 | 630 | 110 | 2 | 6 | 70 | 135 | 68 |
| 2 | 50 | 125 | 45 | 6 | 350 | 135 | 32 |
| 3 | 40 | 135 | 12 | 6 | 630 | 140 | 16 |
| 4 | 60 | 135 | 68 | | | | |

Table 2- Speed and direction of water at different depth in the 2nd expedition.

| Sampling station no. | Depth (cm) | Direction (degree) | Speed (cm/s) | Sampling station no. | Depth (cm) | Direction (degree) | Speed (cm/s) |
|---|---|---|---|---|---|---|---|
| 1 | 50 | 340 | 21 | 4 | 40 | 170 | 5 |
| 1 | 250 | 340 | 32 | 4 | 200 | 265 | 18 |
| 1 | 450 | 340 | 27 | 4 | 450 | 260 | 12 |
| 2 | 50 | 35 | 22 | 5 | 50 | 340 | 11 |
| 2 | 250 | 40 | 37 | 5 | 200 | 335 | 30 |
| 2 | 450 | 40 | 27 | 5 | 450 | 335 | 27 |
| 3 | 80 | 205 | 17 | 6 | 70 | 285 | 40 |
| 3 | 400 | 130 | 41 | 6 | 350 | 325 | 65 |
| 3 | 720 | 130 | 41 | 6 | 630 | 325 | 25 |

Table 3- Speed and direction of water at different depth in the 10th expedition.

| Sampling station no. | Depth (cm) | Direction (degree) | Speed (cm/s) | Sampling station no. | Depth (cm) | Direction (degree) | Speed (cm/s) |
|---|---|---|---|---|---|---|---|
| 1 | 630 | 320 | 38 | 2 | 30 | 290 | 32 |
| 1 | 350 | 305 | 56 | 2 | 60 | 315 | 28 |
| 1 | 70 | 310 | 67 | 3 | 20 | 310 | 35 |
| 2 | 80 | 290 | 22 | | | | |

Table 4-Speed and direction of water at different depth in the 4th expedition.

| Sampling station no. | Depth (cm) | Direction (degree) | Speed (cm/s) | Sampling station no. | Depth (cm) | Direction (degree) | Speed (cm/s) |
|---|---|---|---|---|---|---|---|
| 1 | 540 | 310 | 17 | 3 | 30 | 10 | 13 |
| 1 | 300 | 320 | 19 | 4 | 30 | 340 | 20 |
| 1 | 60 | 350 | 4 | 5 | 50 | 10 | 18 |
| 2 | 180 | 240 | 10 | 6 | 500 | 35 | 17 |
| 2 | 50 | 245 | 18 | 6 | 300 | 5 | 29 |
| 3 | 135 | 280 | 9 | 6 | 60 | 360 | 50 |

*3.1. First expedition April 25, 2003*

Table (1) and Fig.(3-1) showed that the whole water body was moving with a relatively high speed away from the estuary, demonstrating strong ebb conditions (stage 1, Fig.2-a). This was detectable in Fig (4-a) as SSCI index and in Fig. (5-a) as SSC distribution. Water carried bigger particles to the deeper region, and expands width of turbid area. By settlement of bigger particles, the reflectance of water decreased. This could be seen by red tone (with reference to color bar) in the sampling area shown in Fig. (5-a) and lighter tone in Fig. (4-a).

*3.2. Second expedition, May 2, 2003*

Analyzing table (2) and Fig. (3-2), it could be seen that the water body was moving back toward estuary, where the middle part of water (away form both surface and seabed) moved faster. This might represent stage 2 (Fig. 2-b). At this situation, larger particles settled and consequently reflectance of water in a wider area decreased. This could be seen in Fig. (4-b) and Fig. (5-b).

Having compared Figure 4(b) with Fiure 4(a), it could be seen that estuary gets wider ie; more coastal area goes under water. It could also be seen that the SSC distribution in this image was lower in comparison with previous image which proved the occurrence of greater amount of deposition of the sedimentation on the seabed. This would happen twice a day and could be quantified and monitored using remote sensing technology.

*3.3. Tenth expedition, June 18, 2003*

In the beginning of high tide, the estuary was clam, causing the heavier particles to settle faster. But, far from estuary, the whole water body started to move with a high speed (as shown in table 3) toward the river mouth. In accordance to this, Fig. (3-3) showed very high surface current toward estuary, Fig. (4-c) showed a brighter tone proving less surface suspended sediment and Fig. (5-c) showed fresh water approaching the estuary in comparison with the previous images. At this stage, only shallow waters, where the light might reflect from their substrate could be seen turbid. This situation might represent stage 3 shown in Fig. (2-c).

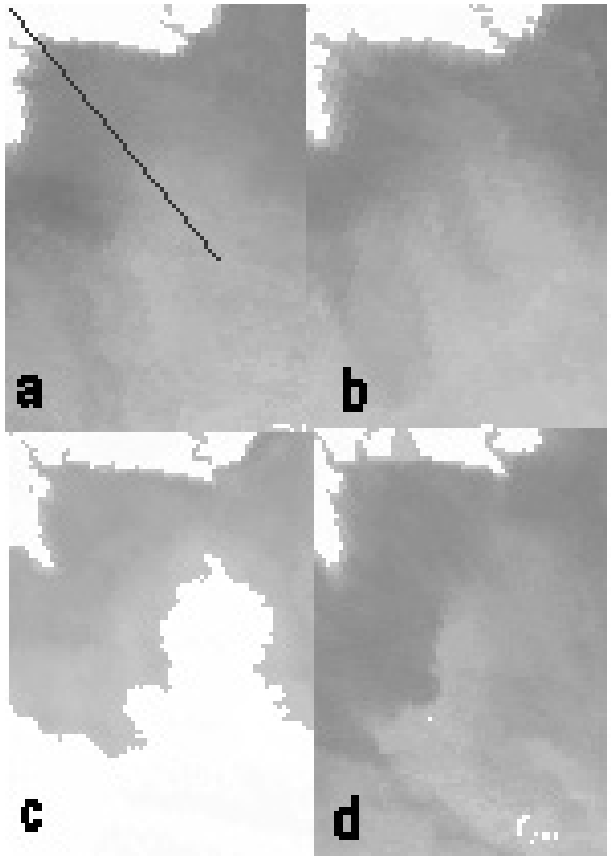


Fig 4. Enlargement of the images produced by SSCI Index for estuary area a)-1st expedition, b)-2nd expedition, c)-10th expedition and d)-4th expedition. A transect for the line is shown in Fig. (6).

*3.4. Fourth expedition, May 29, 2003*

Table (4) and Fig. (3-4) showed that the flood gets to its maturity stage (stage 4, Fig. 2-d). This indicated that the water speed decreased compared to the previous stage, the fresh water interface got as close as possible to the river mouth and the maximum turbidity also approached the river mouth. This could be seen in figures (4-d) and (5-d). Changing surface current direction and low water speed profile caused bigger particles to settle, making average SSC particle size smaller. It could be seen easily at the estuary (Fig. 5-d).

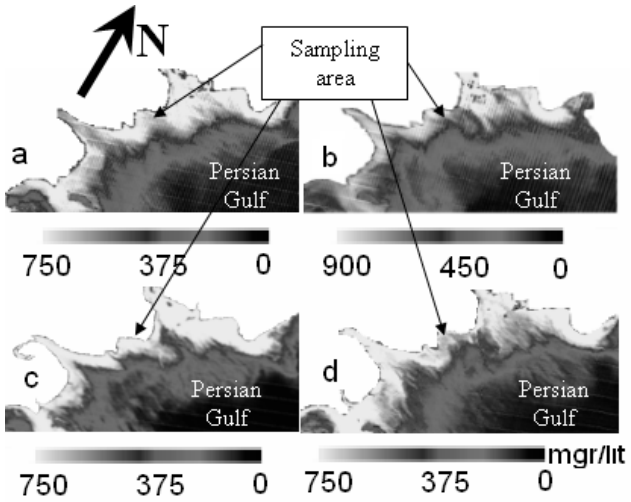


Fig 5. SSC distribution a-1st expedition, b-2nd expedition, c-10th expedition and d-4th expedition (Mobasheri, 2008)

Another way to analyze tidal state at the estuary is to draw a transect line in different directions in the SSCI Index images. As an illustration, this is done in Fig. (4) and the result is shown in figure (6). The vertical axis was the SSCI Index values and the horizontal axis was the relative distance toward the sea. Due to the equal reflectance in channel 1 and 2 for land, SSC Index in this area was almost zero. This is shown in Fig. (6) for the region in the left section of river mouth. On the other hand as the depth increased in shallow waters, the SSCI Index increased irrespective of the tidal stage. This is shown in Fig. (6) for the region between river mouth and the end of shallow waters. In the deeper region, the difference between SSCI Index values for the four different tidal stages would get more detectable. Due to the lower values of SSC at the surface, curve (c) that belongs to the transect of Fig. (4-c), had lower SSCI Index while the other three curves that represent higher turbidities showed more or less the same SSC Index

values as a whole but differ for each case spatially.

## 4. Conclusion

Rivers introduce great amount of sedimentations to the river deltas. Tidal rivers may intensify this phenomenon. Recognition of tidal pattern via SSC may enable one to predict the critical region form sediment deposition points of view. Running algorithm produced by Mobasheri and Mousavi (2004) into first seven MODIS channels may show the distribution of SSC at the very surface in space and time. But, to have a more resolved picture of the phenomenon, an index called SSCI Index proposed by the author proved to be useful. To achieve the ability in quantifying the amount of sediment deposit at each point by using satellite imageries, more in-situ measurements are needed. The authorbelieves that in-situ calibration of SSCI Index on predefined grid nodes may provide a suitable approach for monitoring sedimentation behavior at the critical regions like waters behind the dams.

## 5. Acknowledgement

This author would like to express his gratitude to the Khuzestan Water and Electricity Organization for funding this project and Iran Space Agency for providing MODIS images. I also would like to thank Mr. H. Mousavi and Mr. Ashtari for their hard work in the field. Also many thanks to Khoramshahr Marine Science and Technology University for providing facilities in field campaigns.

## References

Green, M. O., Bell, R. G., Dolphin, T. J. and Swales, A., 2000. Silt and sand transport in a deep tidal channel of a large estuary (Manukau Harbour, New Zealand). Marine Geology. 163: 217-240.

Harris, P. T., 1988. Large-scale bedforms as indicators of mutually evasive sand transport and the sequential infilling of wide-mouthed estuaries. Sedimentary Geology. 57: 273-298.

Li, R. R., Kaufman, Y. J., Gao, Bo-C. and Davis, C. O., 2003. Remote sensing of suspended sediments and shallow coastal waters, IEEE Transaction on Geoscience and Remote sensing, 41: 559.

Mishra, A.K., 2004. Retrieval of suspended sediment concentration in the estuarine waters using IRS-1C WiFS data. International Journal of Applied Earth Observation and Geoinformation. 6: 83–95.

Mobasheri, M. R., 2006. Fundamentals of physics in remote sensing and satellite technology. Farsi Ed., KNToosi University of Technology Publication. 318p.

Mobasheri, M. R. 2008. Assessment of suspended sediments concentration in surface waters, using MODIS images, Am. J. of Applied Sciences, 5(7): 798-804.

Raineya, M.P., Tylera, A.N., Gilveara, D.J., Bryantb, R.G. and McDonald, P., 2003. Mapping intertidal estuarine sediment grain size distributions through airborne remote sensing. Remote Sensing of Environment. 86: 480–490.

Semeniuk, V., 1982. Geomorphology and holocene history of the tidal flats, King Sound, north-western Australia. Journal of the Royal Society of Western Australia. 65: 47-68.

Turner, A., Millward, G.E. and Tyler, A.O., 1994. The distribution and chemical composition of particles in a macrotidal estuary. Estuarine, Coastal and Shelf Science. 38: 1-17.

Wells, J.T., 1995. Tide-dominated estuaries and tidal rivers. In: Perillo, G. M. E., Geomorphology and sedimentology of estuaries. Developments in Sedimentology. 53 :179-205.